nature neuroscience

Neural mechanism underlying complex receptive field properties of motion-sensitive interneurons

Juergen Haag & Alexander Borst

In many species, neurons responding to visual motion at higher processing stages are often specifically tuned to particular flow fields; however, the neural circuitry that leads to this selectivity is not yet understood. Here we have studied this problem in 'vertical system' (VS) cells of the blowfly lobula plate. These neurons possess distinctive local preferred directions in different parts of their receptive field. Dual recordings from pairs of VS cells show that they are electrically coupled. This coupling is responsible for the elongated horizontal extent of their receptive fields. VS cells with a lateral receptive field have additional connections to a VS cell with a frontal receptive field and to the horizontal system, tuning these cells to rotational flow fields. In summary, the receptive field of these cells consists of two components: one that they receive from local motion detectors on their dendrite, and one that they import from other large-field neurons.

Motion-sensitive large-field neurons found at higher processing stages in many species often show large and complex receptive fields: instead of being activated by motion in one direction throughout the receptive field, such neurons respond best to different directions in different locations, giving rise, for example, to expanding or rotating flow fields. Well-studied examples are neurons in area MST in monkeys[1–5], neurons of the accessory optic system in monkeys[6,7] and pigeons[8–11], neurons of the pigeon nucleus rotundus[12], and neurons in the lobula plate of blowflies[13–20]. Across these species, the cells always seem to be intimately involved in the visual control of body posture, eye movement or locomotion. In most cases, however, the neural mechanisms leading to such complex receptive fields have not been clarified. Here we have studied these mechanisms in motion-sensitive neurons in the lobula plate of the blowfly *Calliphora vicina*.

Local motion information in the visual system of the blowfly is processed in separate retinotopically arranged columns[21,22]. This retinotopic order persists through all layers from the photoreceptors to the lobula plate. The lobula plate therefore forms a map of direction-selective small-field elements, where a specific location on the lobula plate corresponds to a particular position in the visual world[13]. It is organized into four direction-specific input layers[23], representing the four main directions of motion. The two anterior layers consist of input elements tuned to horizontal motion (front to back, back to front), whereas the two posterior layers are tuned to vertical motion (upward, downward).

In each hemisphere, the lobula plate contains about 60 individually identifiable motion-sensitive neurons (tangential cells). These tangential cells integrate the output of numerous direction-selective small-field elements on their dendrite[24] and therefore have large receptive fields. Almost all tangential cells respond to visual motion in a direction-selective way[14]. Among these are two subgroups of neurons, 'horizontal system' (HS) cells and VS cells, which are thought to be the principal output elements of the lobula plate. They convey information about large-field horizontal (HS cells) and vertical (VS cells) image motion onto descending neurons, which finally control motor neurons for locomotion or head movements. Both HS and VS cells respond to visual motion stimuli mainly by a graded shift of their membrane potential[25].

The different members (three HS and ten VS cells) of each subgroup occupy different regions in the lobula plate and, owing to the retinotopic organization, have different but often overlapping receptive fields that together almost completely cover the visual space surrounding the animal[26,27]. The VS cells are numbered according to the location of their dendrite in the lobula plate: VS1 has the most lateral dendrite, corresponding to a frontal receptive field; VS10 has the most medial dendrite, corresponding to a caudal receptive field (**Fig. 1c**). Measurements of the receptive field show that these neurons possess different local preferred directions in different parts of their receptive field (refs. 15,16 and **Fig. 1**). This effect is particularly pronounced in the medial VS cells (VS7–VS10), which seem to be tuned more to a rotational than to a translational flow field (**Fig. 1b**): they are maximally excited by upward motion in the frontal part, downward motion in the latero-caudal part, and front-to-back motion in the dorsal part.

Such receptive complex field structures can arise, in principle, through input to the tangential cells from respectively tuned small-field elements. In this situation, because of the retinotopic arrangement of the visual system, the anatomy of the dendrite has to match the receptive field; for example, a neuron that responds to a motion stimulus in the dorsal part of the visual world must have a dendritic branch in the corresponding dorsal part of the lobula plate. For VS

Max-Planck Institute of Neurobiology, Department of Systems and Computational Neurobiology, Am Klopferspitz 18, D-82152 Martinsried, Germany. Correspondence should be addressed to J.H. (haag@neuro.mpg.de).

Published online 9 May 2004; doi:10.1038/nn1245

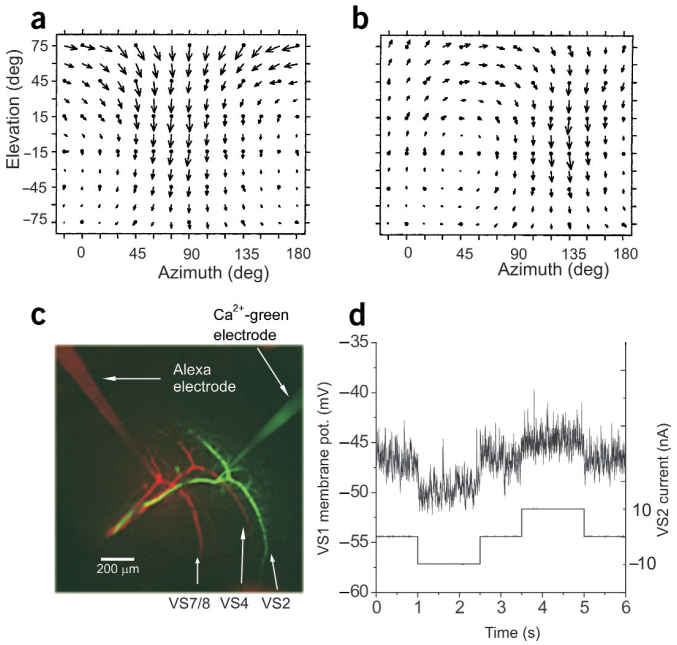

Figure 1 Response characteristics of VS cells. (**a**,**b**) Response fields of VS5 (**a**) and VS8 (**b**) cells. The orientations of the arrows indicate the preferred direction of the cell at this location; the lengths indicate normalized response amplitudes. Both VS5 and VS8 neurons are most prominently sensitive to downward motion, with a peak sensitivity at 90° (VS5) and 135° (VS8), respectively. However, VS5 shows a much broader sensitivity for downward motion than is expected from the anatomy of its dendrite (**a**), and VS8 is sensitive to horizontal motion in the dorsal part and to upward motion in the frontal part of the visual field (**b**). Modified with permission from ref. 16. (**c**) Photograph showing the recording site. Three VS cells are stained: a VS2 cell with Calcium-green, and a VS4 and a VS7/8 cell with Alexa 568. Recordings were made from the axons close to the main branchpoint of the dendrite of VS cells. (**d**) Example of a double recording. Shown is the membrane potential of a VS1 cell recorded while currents of –10 and +10 nA were injected into a VS2 cell.

cells, however, this criterion is not met in a quantitative way: in most VS cells, the sensitivity is broader along the fronto-lateral axis than would be expected from the width of their dendrites. From the area that the dendrites cover in the lobula plate (12–29% for VS2–VS9)[27], the receptive field for most VS cells (VS2–VS8) would be expected to be 30–40° wide. The measured receptive field, however, has been often found[16] to exceed a width of 100° (**Fig. 1a**).

These broad receptive fields contrast with the retinotopic arrangement of the visual system. Obviously, either connections to unknown small-field elements of the lobula plate are involved, or the receptive field structure is altered through network interactions between various VS cells. Because, the lobula plate contains only ten VS cells that can be individually identified in each hemisphere of the blowfly[27], this system lends itself well to a detailed analysis of the mechanisms underlying the flow-field selectivity of motion-sensitive large-field neurons. By investigating the connectivity of VS cells among each other and with HS cells by dual intracellular recordings, here we show that many features of VS-cell receptive fields arise from network interactions between tangential cells.

RESULTS

We first investigated the connectivity between different VS cells in one brain hemisphere. The results of current injections into various VS cells are summarized in **Figure 2**. For simplicity, only the coupling between VS1 and other VS cells (denoted VSx) is shown. The injection of current of –10 nA (**Fig. 2a**) and +10 nA (**Fig. 2b**) into VS1 led to a change in the membrane potential in other VS cells, which shows that all other VS cells are connected to VS1. The coupling strength depended on the vicinity of the respective VS cell to VS1: the closer together the dendrites of the VS cells, the stronger the coupling we found.

The coupling strength as a function of dendritic distance did not, however, tend towards zero for larger distances: for neurons in which the dendrites and the receptive fields were clearly separated (such as VS1 and VS9), a sign reversal occurred. Depolarization of VS1 led to hyperpolarization of VS9, whereas hyperpolarization of VS1 led to depolarization of VS9. The measured gradient in coupling strength was also seen in the reverse experiment in which hyper- and depolarizing currents were injected into various VS cells and the potential change was measured in VS1 (**Fig. 2c**,**d**). Again, the sign reversal was observed for VS1 and VS9.

In addition to the connection between VS1 and the different VS cells, we also found connections between the other VS cells (data not shown). These connections followed the scheme shown in **Figure 2**: the closer together the two VS cells, the stronger the coupling. This strong positive connectivity between neighboring VS cells may form the basis for the broadening of the receptive fields as compared with the width of the dendrite (see Introduction). As **Figure 2** shows, not only is current of both polarities transmitted, but also the connection

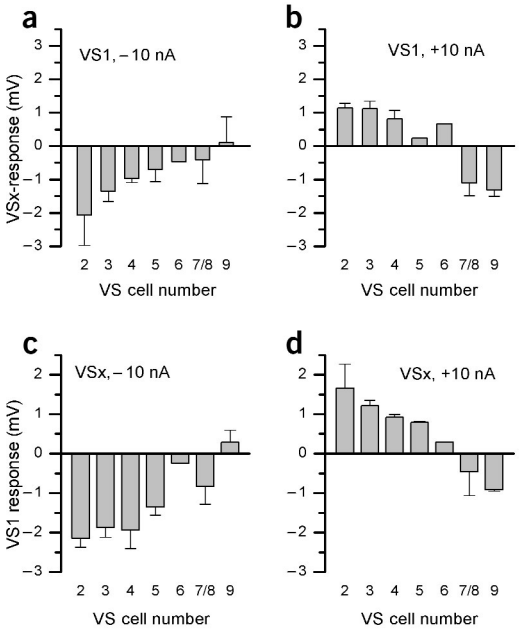

Figure 2 VS cells are electrically coupled. (**a**,**b**) Effects of hyperpolarization (**a**) and depolarization (**b**) of the VS1 cell on the membrane potential of other VS cells (VSx). Current injection into VS1 leads to a change in the membrane potential in VSx cells with the coupling strength dependent on the distance between the respective VSx and VS1 cells. (**c**,**d**) The same gradient can be seen when hyperpolarizing (**c**) or depolarizing (**d**) current is injected into VSx cells and the membrane potential of VS1 is measured. Data are the mean ± s.e.m. of three VS1–VS2, six VS1–VS3, two VS1–VS4, two VS1–VS5, one VS1–VS6, four VS1–VS7/8 and two VS1–VS9 pairs.

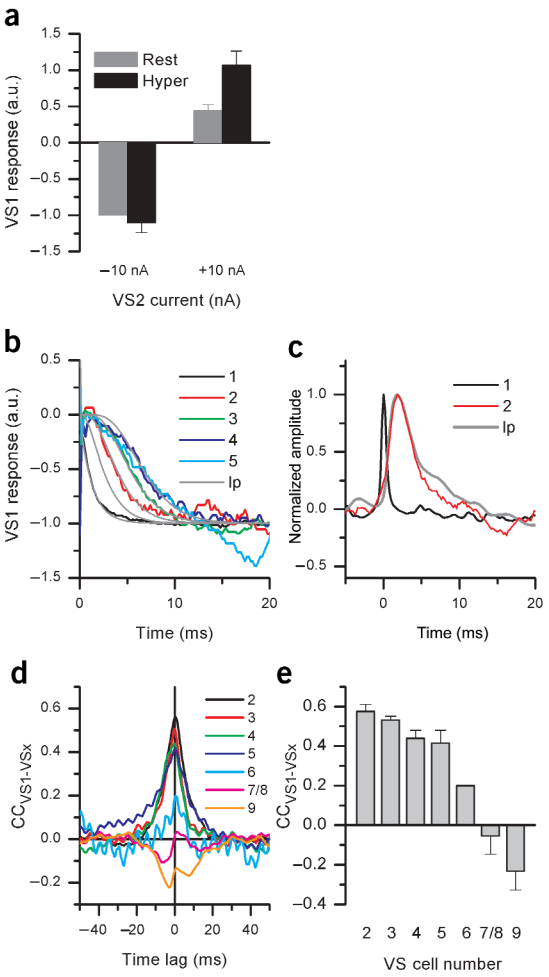

Figure 3 Connectivity between VS cells. (**a**) Constant hyperpolarization of a VS2 cell does not influence the transmission of a hyperpolarizing current step. Gray bars show the relative change in membrane potential in VS1 cells when current steps from 0 nA to –10 nA or +10 nA were injected into a VS2 cell; black bars shows the result when current was stepped from a holding current of –10 nA to –20 nA or 0 nA. The difference in amplitude for the depolarizing current step can be attributed to an outward rectification in VS2 for positive current injections. Data have been normalized to the response amplitude to –10 nA without additional hyperpolarization and show the mean ± s.e.m. over five sweeps for the resting and the hyperpolarized condition. (**b**) Time course of the normalized membrane potential change in VS1 after current injection into various VS cells (VS1–VS5, thick colored lines; for response amplitudes, see **Fig. 2c**). The membrane potential change was averaged over current injections in three VS2, six VS3, two VS4 and two VS5 cells. Thin gray lines show the step response of low-pass filters of increasing order (lp, orders 1–5) with a time-constant of 1.4 ms. (**c**) Spikes in VS1 (black line, amplitude 22.2 mV) used as a trigger to average the membrane potential in VS2 (red line, amplitude 1.3 mV). Gray line shows the convolution of the spikes in VS1 with a second order low-pass filter (time constant 1.4 ms, amplitude 5.2 mV). (**d**) Cross-correlation between the membrane potential (without motion stimulus) of VS1 and that of VSx cells. A strong coupling can be seen for neighboring VS cells, but only a weak or negative coupling for cells that have non-overlapping receptive fields. The positive peak of the cross-correlogram occurs at zero time lag for all cells except VS9. (**e**) Peaks of the correlogram for the different VS cells and VS1. The gradient is the same as that obtained after current injection (**Fig. 2**).

works both ways: current injection into cell 1 leads to a potential change in cell 2, and current injection into cell 2 leads to a potential change in cell 1.

Chemical or electrical synapses

Such a bidirectional connection might be achieved by either electrical or recurrent chemical synapses. For chemical synapses to transmit hyperpolarization, there would have to be a constant release of transmitter at rest that can be downregulated. To distinguish between electrical and chemical synapses, we therefore hyperpolarized one cell with a constant current injection of –10 nA and delivered additional current pulses of –10 and +10 nA. This setup was compared with one without constant hyperpolarization. We considered that if the cell is connected to another cell via chemical synapses, then the steady hyperpolarization should prevent the release of transmitter, and no additional hyperpolarization in response to the current pulse of –10 nA should be seen in the connected cell. If, however, there are electrical synapses between the cells, the additional current pulse of –10 nA should lead to an additional hyperpolarization of the postsynaptic cell.

The result of this experiment is shown in **Figure 3a**. The gray bars show the relative change in membrane potential in VS1 cells when current was stepped from 0 nA to –10 nA or +10 nA; the black bars shows the result when current was stepped from a holding current of –10 nA to –20 nA or 0 nA. There was no difference between the two setups in the response of VS1 to the current pulse of –10 nA, arguing strongly for the presence of an electrical synapse. There was, however, a significant difference between the two setups in the response of VS1 to the current pulse of +10 nA .

This difference can be explained by an outward rectification caused by a potassium conductance in VS cells[25,28]. Owing to the outward rectification, the step from 0 to +10 nA leads to a much smaller potential change in the cell where the current is injected than does the step from –10 to 0 nA, where this outward rectification does not occur. This smaller potential change in the presynaptic cell consequently leads also to a smaller potential change in the coupled cell.

Coupling through electrical synapses cannot, however, explain the negative coupling that occurs between VS1 and VS7/8 and between VS1 and VS9 cell pairs (**Fig. 2**). Because there is a sign reversal in the response (for example, depolarization of VS1 leads to hyperpolarization of VS7/8 and VS9), there must be a connection via chemical synapses between the two cells.

Wiring schemes

The gradient in the coupling strength might be explained by two different wiring schemes of the VS cells: first, each VS cell is directly connected to all other VS cells but the connection strength varies according to the location of the dendritic tree; second, each VS cell is connected only to its immediate neighbor cells. In the second scheme, for example, there is no direct connection between VS1 and VS3, but current injection into VS3 changes the membrane potential in VS2, and VS2 transmits this potential change to VS1.

To distinguish between these two wiring schemes, we analyzed the time course of the voltage changes. The time course of the normalized membrane potential of VS1 when hyperpolarizing current was injected into various VS cells is shown in **Figure 3b**. The black line shows the result of a double recording from a VS1 cell, where one electrode was located in the lobula plate arbor of the cell and the second was placed in the axon near the terminal region of the same cell. This enabled us to extract the time constant of the intracellular transfer function by fitting the time course with a single exponential decay (first-order low-pass) with a time constant of 1.4 ms.

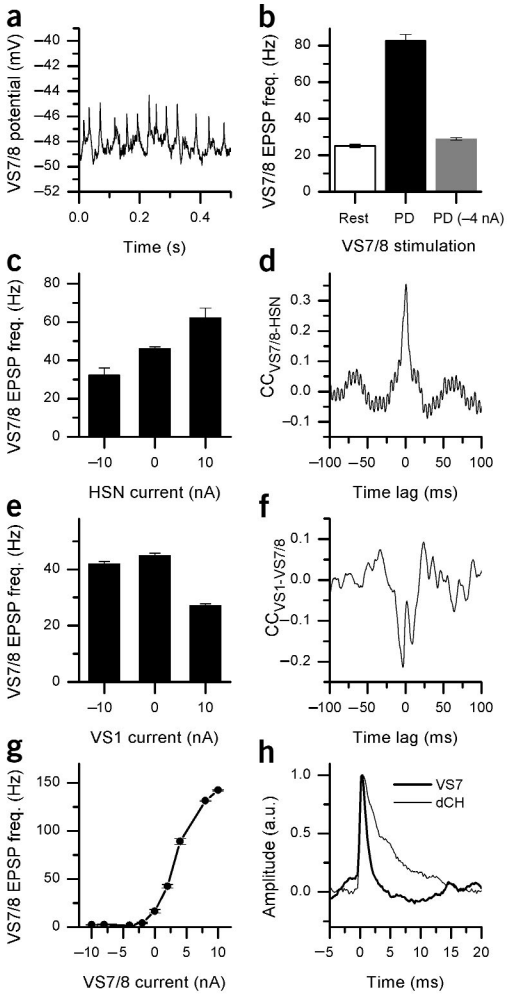

Figure 4 EPSP analysis in VS7/8. (**a**) EPSPs recorded in VS7/8. (**b**) Horizontal motion stimuli increase the EPSP frequency (black bar). When the motion stimulus was paired with an injection of hyperpolarizing current of –4 nA into a VS7/8 cell (gray bar), the current injection counteracted the effect of the motion stimuli in VS7/8 by reducing to about resting levels (white bar) the increase in EPSP frequency that occurs during preferred direction motion. Data are the mean ± s.e.m. over ten sweeps. (**c**–**f**) Hyperpolarization of HSN decreases the frequency and depolarization increases the frequency of EPSPs in VS7/8 (**c**); by contrast, depolarization of VS1 decreases the frequency of EPSPs (**e**). These opposing effects can also be seen in the correlograms: HSN and VS7/8 membrane potentials are positively correlated (**d**), whereas VS1 and VS7/8 are negatively correlated (**f**). Data are the mean ± s.e.m. over five sweeps. (**g**) Direct current injection into VS7/8 alters the frequency of the measured EPSPs. (**h**) Comparison of the shape of EPSPs in VS7/8 (thick line) with EPSPs elicited by H1 in a dCH cell (thin line). Note that the decay of the membrane potential is much faster in VS7/8 than in dCH.

The time course of the membrane potential change in VS1 was much slower when current was injected into other VS cells. The different traces could be fitted with low-pass filters of higher orders. When current was injected into VS2, the resulting membrane potential change in VS1 was best described by a third-order low-pass; when current was injected into VS3, it was best described by a fourth-order low-pass filter; and so on. For current injection into VS5, however, the exact order of the low-pass filter fitting the response best was hard to quantify, owing to the small signal-to-noise ratio of the response.

The increase in the order of the low-pass filter indicates the presence of a coupling chain. It seems that each VS cell is not directly connected to all other VS cells, but is connected only indirectly via its immediate neighbors. Thus, current injection into one cell changes the membrane potential in the neighboring cell, which is propagated to a third cell, and so on.

We found that not only hyper- or depolarizing current steps, but also action potentials occurring in VS1 are transmitted between VS cells (**Fig. 3c**). In **Figure 3c**, the black trace shows the averaged spike elicited in VS1, whereas the red trace shows the spike-triggered average of the response in a simultaneously recorded VS2 cell. Spikes in VS1 resulted in excitatory postsynaptic potentials (EPSPs) in VS2 that were delayed by about 2 ms, showing that fast potential changes are transmitted between VS1 and VS2. In the current injection experiments, the response of VS2 to a current injection into VS1 was best fitted with a third-order low-pass filter. In this experiment, however, the potential change in VS2 was compared with the potential change in VS1 and not with the current step, and thus the resulting potential change in VS2 was fitted with a second-order low-pass filter. This finding is in agreement with the results from the current injections because no intracellular transfer function (a first-order low-pass filter) for VS1 needs to be considered.

The effect of the coupling was also visible in the cross-correlogram between different VS cells and VS1 (**Fig. 3d,e**). For VS cells with their dendrite next to the dendrite of VS1, there was a strong positive correlation that peaked at zero time lag (**Fig. 3d**). The correlation between VS1 and VS7/8 and between VS1 and VS9 turned negative. The plot of the correlation peaks for the different VS cells and VS1 (**Fig. 3e**) showed the same gradient as that obtained from the current injections (**Fig. 2**).

Taken together, these data indicate that the VS cells are coupled via electrical synapses. This coupling of VS cells can explain the broad receptive fields of VS cells (**Fig. 1a**). Accordingly, the measured receptive field of the VS cells reflects a superposition of direct and indirect input. The direct input comes from motion-sensitive small-fields elements synapsing onto the dendrite; this component therefore correlates with the anatomical location of the dendrite. The indirect input comes from neighboring VS cells and is imported through electrical connections.

VS cells with a lateral receptive field

The coupling among VS cells cannot, however, account for the strong sensitivity of VS cells with a lateral receptive field (VS7–VS9) to horizontal motion in the dorsal part of the receptive field (ref. 16 and **Fig. 1b**). The membrane potential of these cells showed distinct EPSPs (**Fig. 4a**). Horizontal motion increased the frequency of these EPSPs to about 83 Hz (**Fig. 4b**, filled bar) from the resting frequency of 29 Hz (**Fig. 4b**, open bar). Thus, in addition to local motion detector input that results in a graded potential shift, VS7/8 cells must receive input from a spiking interneuron that is sensitive to horizontal motion.

Because the preferred direction of this spiking neuron matched the preferred direction of HS cells, we tested whether the EPSP frequency in VS7/8 could be altered by current injection into HS cells by making dual intracellular recordings of HSN (horizontal system north) and VS7/8. Depolarization and hyperpolarization of HSN decreased and increased, respectively, the frequency of EPSPs in VS7/8 (**Fig. 4c**). This influence could be also seen in the correlation between HSN and VS7/8, where a positive correlation at zero time lag occurred (**Fig. 4d**). Because the anatomy of this spiking neuron has not been determined, below we refer to it as 'X'.

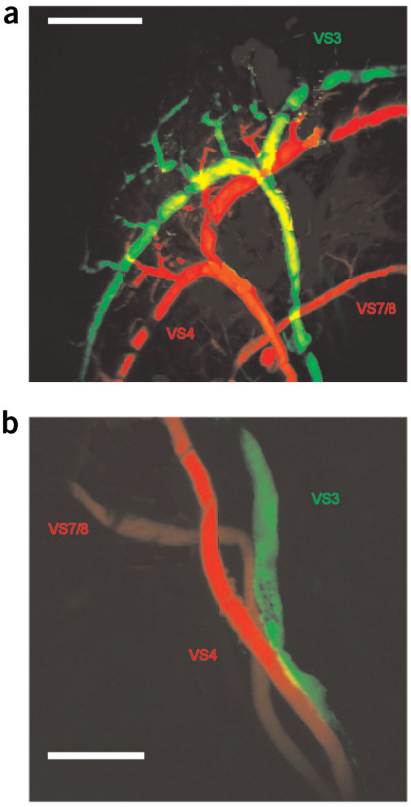

Figure 5 Two-photon imaging of VS cells. Shown are a VS3 cell stained with Calcium-green, and a VS4 and a VS7/8 cell stained with Alexa 568. (**a**) Low magnification image of the dendrites oriented to correspond to a frontal section (scale bar, 100 μm). (**b**) Image of the axons of the three VS cells (scale bar, 50 μm). They run in close vicinity to each other, facilitating direct contact.

In contrast to HSN cells, VS1 decreased the frequency of EPSPs in VS7/8 and VS9 (**Fig. 4e**). Whereas hyperpolarization of VS1 did not alter the frequency of EPSPs in VS7/8, depolarization of VS1 reduced the EPSP frequency from 45 Hz to 27 Hz. In addition to the effect on the frequency of EPSPs, there was also a direct inhibition of VS1 onto VS7/8 and VS9 that could be seen in the graded potential shift after depolarization of VS1 (**Fig. 2b**). In contrast to the VS7/8-HSN cross-correlogram, the correlation peak between VS7/8 and VS1 was negative (**Fig. 4f**), again indicating the inhibition of VS1 and VS7/8.

The frequency of EPSPs in VS7/8 could be altered not only by current injection into VS1 or HSN, but also by direct current injection into VS7/8 itself (**Fig. 4g**). This current injection had a more pronounced effect than did injection into HSN or VS1. Hyperpolarization of VS7/8 reduced the EPSP frequency to almost 0 Hz, whereas depolarization with 10 nA increased the frequency to 140 Hz (**Fig. 4g**). Simultaneous horizontal motion stimulation and a negative current injection of –4 nA into the axon of VS7/8 showed that the increase in EPSP frequency during the motion stimulus could be suppressed by hyperpolarization of VS7/8 (**Fig. 4b**, gray bar).

The fact that the frequency of EPSPs recorded in the VS7/8 could be altered by current injection into VS7/8 pointed towards a connection via electrical synapses between VS7/8 and the spiking neuron (X) responsible for the EPSPs. Comparison of the shape of the EPSPs in VS7/8 with the shape of EPSPs measured in a dCH (dorsal centrifugal horizontal) cell showed that the EPSPs in VS7/8 have a much shorter decay time (**Fig. 4h**). It is therefore likely that these fast deflections of the membrane potential are not EPSPs caused by chemical transmission but rather are passive reflections of action potentials occurring in the spiking neuron.

Site of contact

We used two-photon microscopy to determine where the different VS cells contact their neighboring VS cells. We filled VS cells with two fluorescent dyes (Calcium-green and Alexa 568) to identify possible contact sites between the cells. The dendrites of neighboring neurons (such as VS1 and VS2) showed some overlap (data not shown), but even using high-magnification images we could not establish whether two cells make dendritic contacts with each other.

By contrast, we found no areas where the dendrites of non-neighboring VS cells (such as VS1 and VS7) overlap. For these cell pairs, it can be excluded that they contact each other via their dendrites. Another area where the different VS cells came close to each other was the axons of the cells. The axons of three different VS cells, a VS3 cell filled with Calcium-green, and a VS4 and a VS7/8 cell filled with Alexa 568, are shown in **Figure 5**. These three cells overlapped anatomically along their axons, indicating that VS cells may contact neighboring VS cells through axo-axonal connections.

DISCUSSION

Our results show that VS cells are connected to each other. The coupling strength depends on the relative distance between the cells' dendrites: the closer together the dendrites are, the stronger the coupling is. This finding can explain the unexpected broad receptive field of most VS cells, which substantially exceeds the area of dendritic coverage in the lobula plate.

The strength of the coupling between neighboring VS cells is, however, weak: hyperpolarization with a current injection of –10 nA, which results in a shift of about –30 to –40 mV in the injected cell, led to a hyperpolarization in the neighboring cell of only about –2 mV (5%). If our hypothesis of a sequential VS-cell connection is correct, and if a loss of 95% of the original potential were to be continued through the chain of VS cells, there would be no effect left in the cell next to the neighboring cell, in other words, after two steps.

Most probably, however, the measured drop in potential does not reflect the real coupling strength between two VS cells. In explanation of the small response, one has to consider the fact that both electrodes were positioned near the branchpoint of the dendrites (see **Fig. 1c**). If the cells contact each other near the terminal region, the measured signal will be attenuated not only at the contact between the cells, but also twice along the axons of the two cells. An indication that this attenuation indeed may be the main reason for the small responses comes from the calculation of the spike-triggered average (**Fig. 3c**). In this experiment, the spikes occurring in VS1 were used as a trigger for averaging the membrane potential of VS2. Because the action potentials in VS1 are conducted to the terminal region by active processes, the potential measured at the recording site and at the site where the connection is made are roughly identical. In this situation, the measured potential in VS2 is about 25% of the expected value and thus five times higher than that measured with current injection. Such axo-axonal coupling of neurons has been shown for hippocampal pyramidal cells and has been discussed as a mechanism for a fast neuronal communication[29].

Coupling through electrical synapses does not explain the sign reversal found for VS1 and VS7–VS9. To explain these effects, chemical synapses between these cells must be postulated. The effects of such mixed synapses can be seen in the time course of the cross-

correlograms. The cross-correlograms between VS7/8 or VS9 and VS1 (**Figs. 3d** and **4f**) showed a positive peak at zero time lag with a flanking negative part; thus, they seem to reflect the existence of two separate connections: an excitatory one with a narrow positive peak, and an inhibitory one with a broader negative peak. The positive peak can be explained by an electrical coupling of neighboring VS cells; in addition, there must be a chemical inhibitory coupling of VS1 and VS7–VS9. Such mixed synapses have been shown, for example, in the pyloric network of the spiny lobster[30].

As well as their primary receptive field owing to direct retinotopic input from local motion-sensitive elements, VS cells import the receptive field of their direct neighbors through the connectivity between them. Although such neighborhood connectivity is found for all VS cells, cells with a lateral receptive field show a most interesting tuning for rotational flow fields. Our experiments showed that VS cells receive graded excitatory input from neighboring VS cells. For VS7/8 cells, this input is from VS6 and from VS9. It leads to a broadening of the receptive field along the fronto-caudal axis (**Supplementary Fig. 1** online). In addition, the number of EPSPs occurring in VS7/8 is influenced by two cells: VS1 and HSN. This influence, however, is opposing: whereas depolarization of VS1 decreases the frequency of EPSPs (**Fig. 4e**), depolarization of HSN increases the frequency (**Fig. 4b**).

The effect of VS1 on the frequency of the EPSPs measured in VS7/8 cannot be direct, because VS1 cells are not firing action potentials in a regular way. Rather, we postulate that VS1 acts on VS7/8 via an electrical coupling of VS7/8 with the spiking neuron responsible for the EPSPs. Depolarization of VS1 leads to hyperpolarization of VS7/8 and, because of the electrical coupling, a decrease in EPSP frequency. Because VS1 is depolarized by upward motion in the frontal part of the receptive field, VS7/8 becomes hyperpolarized by frontal motion stimuli. This process explains the sensitivity for upward motion of VS7/8 in the frontal part (**Supplementary Fig. 1** online). The sensitivity of VS7/8 to horizontal front-to-back motion in the dorsal part (**Supplementary Fig. 1** online) is mediated by an excitatory connection to HSN. Because there is no graded shift in membrane potential in VS7/8 on hyper- or depolarization of HSN, this connection is not direct but occurs through a spiking neuron (X). So far, this spiking neuron has not been identified anatomically. The direct current injection into VS7/8 shows that VS7/8 are coupled to this spiking neuron with electrical synapses.

In summary, our experiments show that the complex receptive field of VS cells of the fly visual system is only partially due to direct input from local motion-sensitive elements. In addition, many features of the receptive fields are imported through network interactions from other tangential cells. Such a wiring scheme might represent an evolutionary advantage, because only a few, simple developmental rules are needed. In particular, for axo-axonal coupling, the receptive fields of connected tangential cells can be completely imported with only a single connection. If these receptive fields were built up by connecting the VS cells to appropriately tuned small-field elements, or if the VS cells were to contact each other at multiple dendritic sites, the wiring would be much more complicated.

In future experiments we plan to ablate individual neurons selectively by filling them with fluorescent dye and illuminating them by strong laser light[31]. Applying such techniques to the elements of the circuit, we hope to unravel the primary receptive field of VS cells without the contribution of the network.

METHODS

Preparation and setup. Female blowflies (*C. vicina*) were dissected as described[25] and mounted on a heavy recording table looking down onto the stimulus monitors. We viewed the fly brain from behind through a fluorescence microscope (Axiotech Vario 100 HD, Zeiss).

Stimulation. Stimuli were generated on Tektronix 608 monitors by an image synthesizer (Picasso, Innisfree) and consisted of a one-dimensional grating of 16.7° spatial wavelength and 87% contrast, displayed at a frame rate of 200 Hz. The mean luminosity of the screen was 11.2 cd/m^2. The intensity of the pattern was square-wave modulated along its horizontal axis. The stimulus field extended from 16° to 42° for the left eye and from 16° to 48° for the right eye along the horizontal axis, and from –30° to +30° along the vertical axis of the fly.

Electrical recording. For intracellular recordings, we pulled electrodes on a Brown-Flaming micropipette puller (P-97) using thin-wall glass capillaries with an outer diameter of 1 mm (Clark, GC100TF-10), which resulted in resistances of about 15 MΩ. One electrode was filled with the green fluorescent dye Calcium-green, the other was filled with the red fluorescent dye Alexa 568 (both from Molecular Probes). The output signals of two SEL10-amplifiers (npi-electronics) were fed to a Pentium III PC via a 12-bit A/D converter (DAS-1602/12, Computerboards) at a sampling rate of 5 kHz and stored to hard disc. Recordings were made from VS cell axons. For most cells, the electrodes were placed near the main branchpoint of the dendrite (**Fig. 1c**). Because VS7 and VS8 are hard to distinguish, we averaged the responses of these two neurons and referred to them as VS7/8.

Signals were evaluated off-line by programs written in Delphi (Borland). EPSPs in the intracellular recorded responses were detected by taking the derivative of the response and applying a threshold operation (**Fig. 4**). We calculated the normalized cross-correlogram (**Fig. 3d,e**) from the first 800 ms of the membrane potentials in the following way. Defining the cross-correlation (CC) between two responses r_A and r_B (with T as period length and τ as time delay) as

$$CC(\tau) = \left\langle \frac{1}{T} \int_0^T dt \cdot r_A(t) \cdot r_B(t+\tau) \right\rangle$$

and the total power of $r_X(t)$ as

$$\sigma_X^2 = \left\langle \frac{1}{T} \int_0^T dt \cdot r_X^2(t) \right\rangle,$$

the normalized cross-correlation[32], $h(\tau)$, is then

$$h(\tau) = \frac{CC(\tau)}{\sqrt{\sigma_A^2 \cdot \sigma_B^2}}.$$

Two-photon microscopy. We used a custom-built two-photon microscope and a 5W-pumped Ti:sapphire laser (MaiTai, Spectra Physics). For details, see refs. 33,34.

Note: Supplementary information is available on the Nature Neuroscience website.

ACKNOWLEDGMENTS

We are grateful to R. Gleich for excellent technical assistance. This work was supported by the Max-Planck-Society.

COMPETING INTERESTS STATEMENT

The authors declare that they have no competing financial interests.

Received 29 December 2003; accepted 29 March 2004
Published online at http://www.nature.com/natureneuroscience/

1. Lappe, M., Bremmer, F., Pekel, M., Thiele, A. & Hoffmann, K.P. Optic flow processing in monkey STS: a theoretical and experimental approach. *J. Neurosci.* **16**, 6265–6285 (1996).
2. Tanaka, K. & Saito, H. Analysis of motion of the visual field by direction, expansion/contraction, and rotation cells clustered in the dorsal part of the medial superior temporal area of the macaque monkey. *J. Neurophysiol.* **62**, 626–641 (1989).
3. Duffy, C.J. & Wurtz, R.H. Sensitivity of MST neurons to optic flow stimuli. I. A con-

tinuum of response selectivity to large-field stimuli. *J. Neurophysiol.* **65**, 1329–1345 (1991).
4. Duffy, C.J. & Wurtz, R.H. Sensitivity of MST neurons to optic flow stimuli. II. Mechanisms of response selectivity revealed by small-field stimuli. *J. Neurophysiol.* **65**, 1346–1359 (1991).
5. Duffy, C.J. & Wurtz, R.H. Medial superior temporal area neurons respond to speed patterns in optic flow. *J. Neurosci.* **17**, 2839–2851 (1997).
6. Hoffmann, K.P. & Distler, C. Quantitative analysis of visual receptive fields of neurons in nucleus of the optic tract and dorsal terminal nucleus of the accessory optic tract in macaque monkey. *J. Neurophysiol.* **62**, 416–428 (1989).
7. Hoffmann, K.P., Bremmer, F., Thiele, A. & Distler, C. Directional asymmetry of neurons in cortical areas MT and MST projecting to the NOT-DTN in macaques. *J. Neurophysiol.* **87**, 2113–2123 (2002).
8. Crowder, N.A., Lehmann, H., Parent, M.B. & Wylie, D.R. The accessory optic system contributes to the spatio-temporal tuning of motion-sensitive pretectal neurons. *J. Neurophysiol.* **90**, 1140–1151 (2003).
9. Crowder, N.A., Dawson, M.R. & Wylie, D.R. Temporal frequency and velocity-like tuning in the pigeon accessory optic system. *J. Neurophysiol.* **90**, 1829–1841 (2003).
10. Gu, Y., Wang, Y. & Wang, S.R. Directional modulation of visual responses of pretectal neurons by accessory optic neurons in pigeons. *Neuroscience* **104**, 153–159 (2001).
11. Wylie, D.R. & Frost, B.J. Responses of neurons in the nucleus of the basal optic root to translation and rotational flowfields. *J. Neurophysiol.* **81**, 267–276 (1999).
12. Wang, Y. & Frost, B.J. Time to collision is signaled by neurons in the nucleus rotundus of pigeons. *Nature* **356**, 236–238 (1992).
13. Hausen, K. Monocular and binocular computation of motion in the lobula plate of the fly. *Verh. Dtsch. Zool. Ges.* **74**, 49–70 (1981).
14. Hausen, K. The lobula-complex of the fly: structure, function and significance in visual behaviour. In *Photoreception and Vision in Invertebrates* (ed. Ali, M.A.) 523–559 (Plenum, New York, 1984).
15. Krapp, H.G. & Hengstenberg, R. Estimation of self-motion by optic flow processing in single visual interneurons. *Nature* **384**, 463–466 (1996).
16. Krapp, H.G., Hengstenberg, B. & Hengstenberg, R. Dendritic structure and receptive-field organization of optic flow processing interneurons in the fly. *J. Neurophysiol.* **79**, 1902–1917 (1998).
17. Krapp, H.G., Hengstenberg, R. & Egelhaaf, M. Binocular contributions to optic flow processing in the fly visual system. *J. Neurophysiol.* **85**, 724–734 (2001).
18. Haag, J. & Borst, A. Recurrent network interactions underlying flow-field selectivity of visual interneurons. *J. Neurosci.* **21**, 5685–5692 (2001).
19. Haag, J. & Borst, A. Orientation tuning of motion-sensitive neurons shaped by vertical-horizontal network interactions. *J. Comp. Physiol.* **189**, 363–370 (2003).
20. Borst, A. & Haag, J. Neural networks in the cockpit of the fly. *J. Comp. Physiol.* **188**, 419–437 (2002).
21. Strausfeld, N.J. Functional neuroanatomy of the blowfly's visual system. In *Photoreception and Vision in Invertebrates* (ed. Ali, M.A.) 483–522 (Plenum, New York, 1984).
22. Bausenwein, B., Dittrich, A.P. & Fischbach, K.F. The optic lobe of *Drosophila melanogaster*. II. Sorting of retinotopic pathways in the medulla. *Cell Tissue Res.* **267**, 17–28 (1992).
23. Buchner, E. & Buchner, S. Mapping stimulus-induced nervous activity in small brains by [H]2-deoxy-D-glucose. *Cell Tissue Res.* **211**, 51–64 (1980).
24. Single, S. & Borst, A. Dendritic integration and its role in computing image velocity. *Science* **281**, 1848–1850 (1998).
25. Haag, J., Theunissen, F. & Borst, A. The intrinsic electrophysiological characteristics of fly lobula plate tangential cells. II. Active membrane properties. *J. Comput. Neurosci.* **4**, 349–369 (1997).
26. Hausen, K. Motion sensitive interneurons in the optomotor system of the fly. II. The horizontal cells: receptive field organization and response characteristics. *Biol. Cybern.* **46**, 67–79 (1982).
27. Hengstenberg, R., Hausen, K. & Hengstenberg, B. The number and structure of giant vertical cells (VS) in the lobula plate of the blowfly *Calliphora erytrocephala*. *J. Comp. Physiol. A* **149**, 163–177 (1982).
28. Haag, J. & Borst, A. Amplification of high-frequency synaptic inputs by active dendritic membrane processes. *Nature* **379**, 639–641 (1996).
29. Schmitz, D. *et al.* Axo-axonal coupling: a novel mechanism for ultrafast neuronal communication. *Neuron* **31**, 831–840 (2001).
30. Mamiya, A., Manor, Y. & Nadim, F. Short-term dynamics of a mixed chemical and electrical synapse in a rhythmic network. *J. Neurosci.* **23**, 9557–9564 (2003).
31. Farrow, K., Haag, J. & Borst, A. Input organization of multifunctional motion sensitive neurons in the blowfly. *J. Neurosci.* **23**, 9805–9811 (2003).
32. Kimpo, R.R., Theunissen, F.E. & Doupe, A.J. Propagation of correlated activity through multiple stages of a neural circuit. *J. Neurosci.* **23**, 5750–5761 (2003).
33. Denk, W., Strickler, J.H. & Webb, W.W. Two-photon laser scanning fluorescence microscopy. *Science* **248**, 73–76 (1990).
34. Borst, A., Denk, W. & Haag, J. *In vivo* calcium imaging in the fly visual system. in: *Imaging Living Cells: A Laboratory Manual* 2nd edn (eds. Yuste, R., Lanni, F. & Konnerth, A.) Ch. 44 (CSHL, Cold Spring Harbor, NY, 2004).